The EUMETSAT Network of Satellite Application Facilities

ROM SAF
Radio Occultation Meteorology

Two methods of electron density retrieval from truncated ionospheric radio occultation data

Haixia Lyu(1,2), Manuel Hernández-Pajares(1,2), Enric Monte-Moreno(3), Estel Cardellach(1,4)

1) IEEC, Barcelona, Spain 2) UPC-IonSAT, Barcelona, Spain
3) UPC-TALP, Barcelona, Spain 4) ICE-CSIC, Barcelona, Spain

EUMETSAT ROM SAF - IROWG2019

Konventum, Helsingør (Elsinore), Denmark, 19 - 25 September 2019

The EUMETSAT Network of Satellite Application Facilities
ROM SAF
Radio Occultation Meteorology

Outline

1. Background
2. Method 1: SEEIRO
3. Method 2: AVHIRO
4. Assessment
5. Conclusions

1. Background

Goal and context

- ✓ The new EUMETSAT Polar System 2nd Generation (EPS-SG) satellites are designed for neutral atmospheric sounding. The orbit height is in the range 823-848 km.
- ✓ EPS-SG, will provide as well an opportunity of ionospheric sounding, with impact parameter height only below 500km.

1. Background

Goal and context

- ✓ The new EUMETSAT Polar System 2nd Generation (EPS-SG) satellites are designed for neutral atmospheric … the range 823-848 km

Blind area between 500 km and orbit height

- ✓ EPS-SG, will provide as well an opportunity of ionospheric sounding, with impact parameter height only below 500km.

1. Background

Goal and context

- ✓ The new EUMETSAT Polar System 2nd Generation (EPS-SG) satellites are designed for neutral atmospheric … the range 823-848 km
- ✓ EPS-SG, will provide as well an opportunity of ionospheric sounding, with impact parameter height only below 500km.

Blind area between 500 km and orbit height

Extrapolation

1. Background

Goal and context

- ✓ The new EUMETSAT Polar System 2nd Generation (EPS-SG) satellites are designed for neutral atmospheric ... the range 823-848 km

Blind area between 500 km and orbit height

- ✓ EPS-SG, will provide as well an opportunity of ionospheric sounding, with impact parameter height only below 500km.

Previous work

Extrapolation

- ✓ The Vary-Chap model where the scale height varies linearly with respect to height has been proposed based on FORMOSAT-3/COSMIC GPS occultation data inverted by means of the Improved Abel transform inversion technique, taking into account the horizontal electron content gradients (Olivares-Pulido et al., 2016)
- ✓ A new electron density extrapolation technique - the Vary-Chapman Extrapolation Technique (VCET) - for impact parameters of 500km up to the EPS-SG orbit height was developed, when accurate electron density profile below 500km is available (Hernández-Pajares et al., 2017)

The Vary-Chapman Extrapolation Technique (VCET)

$Nm, hm, H_{o,t}, \partial H_t/\partial h$

$$N = N_m e^{k(1-z-e^{-z})}, \text{ where } z = \frac{h-hm}{H}$$

$$H_t(h) = \frac{\partial H_t}{\partial h}(h - h_m) + H_{0,t}\ , h \geq h_m$$

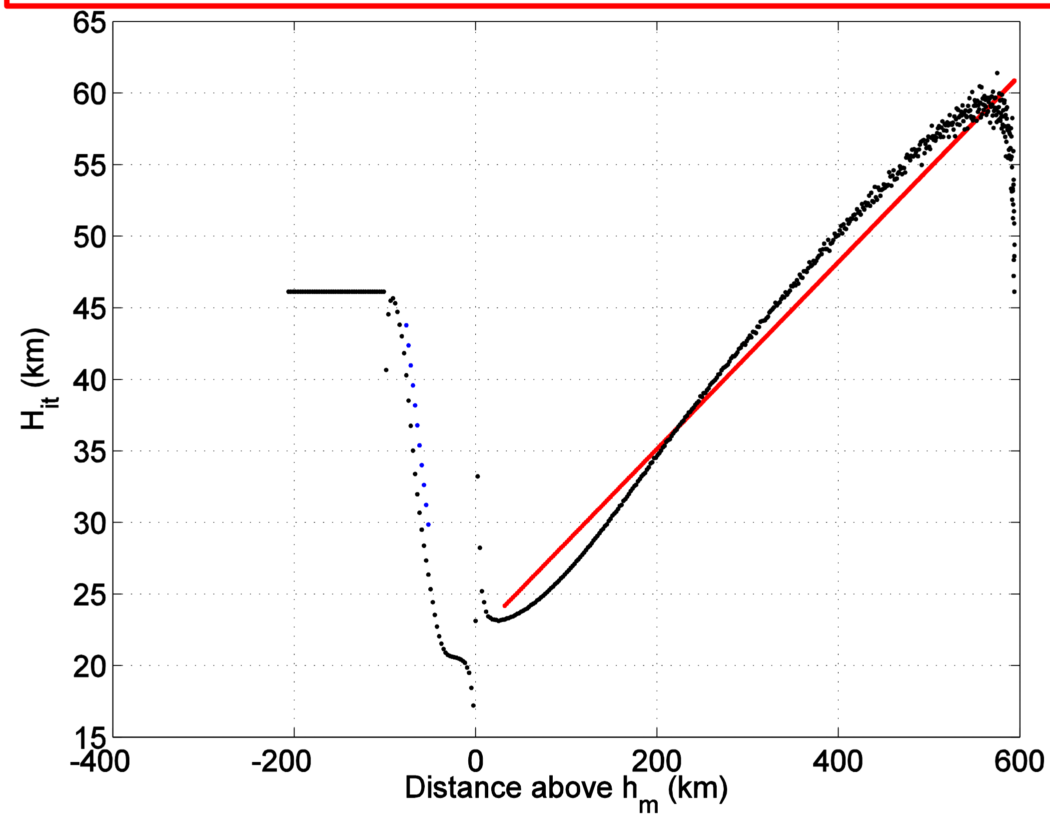

2. Method 1: SEEIRO

the Simple Estimation of Electron density profiles from topside Incomplete RO data

2. Method 1: SEEIRO

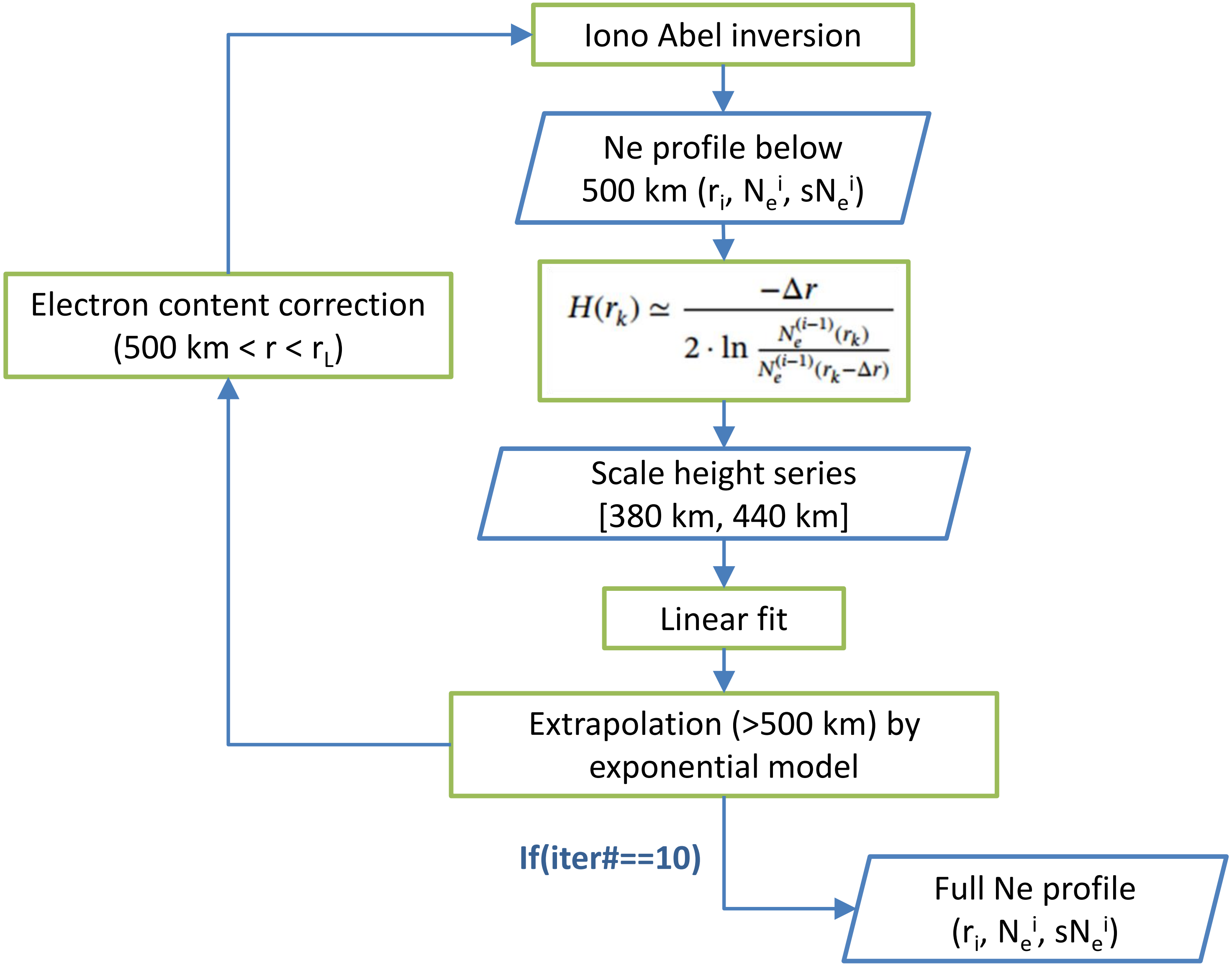

2. Method 1: SEEIRO

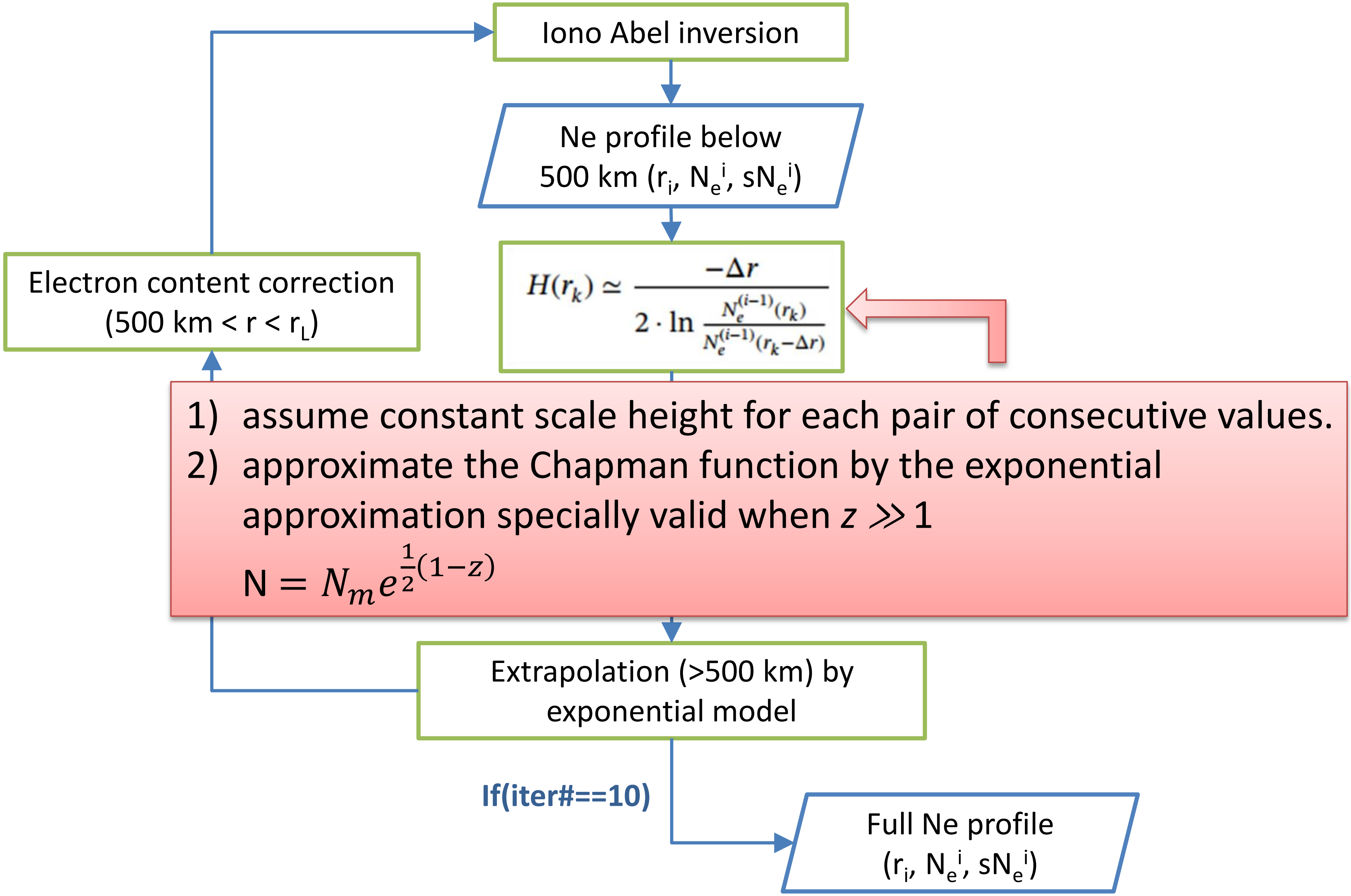

ROM SAF
Radio Occultation Meteorology

2. Method 1: SEEIRO

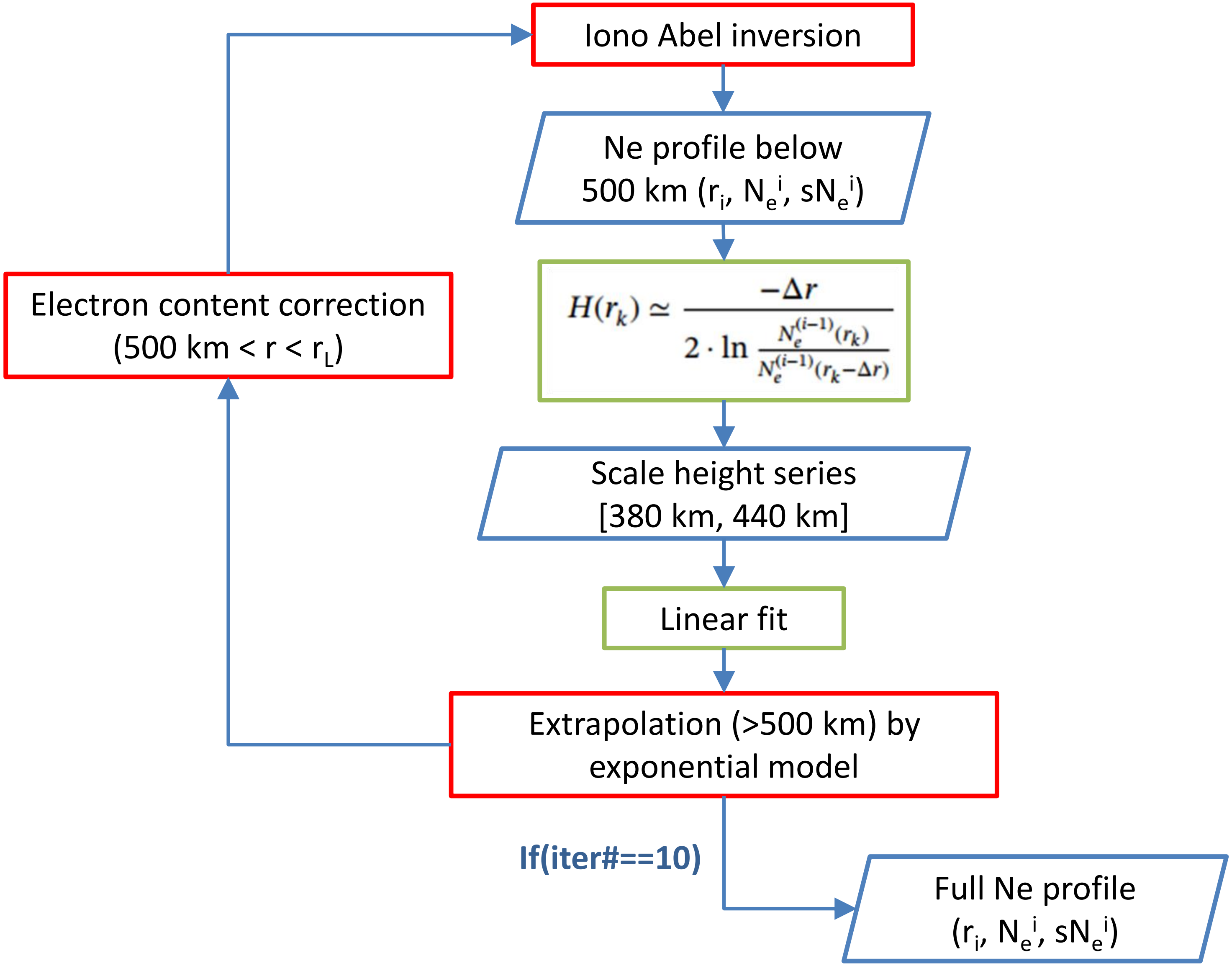

2. Method 1: SEEIRO

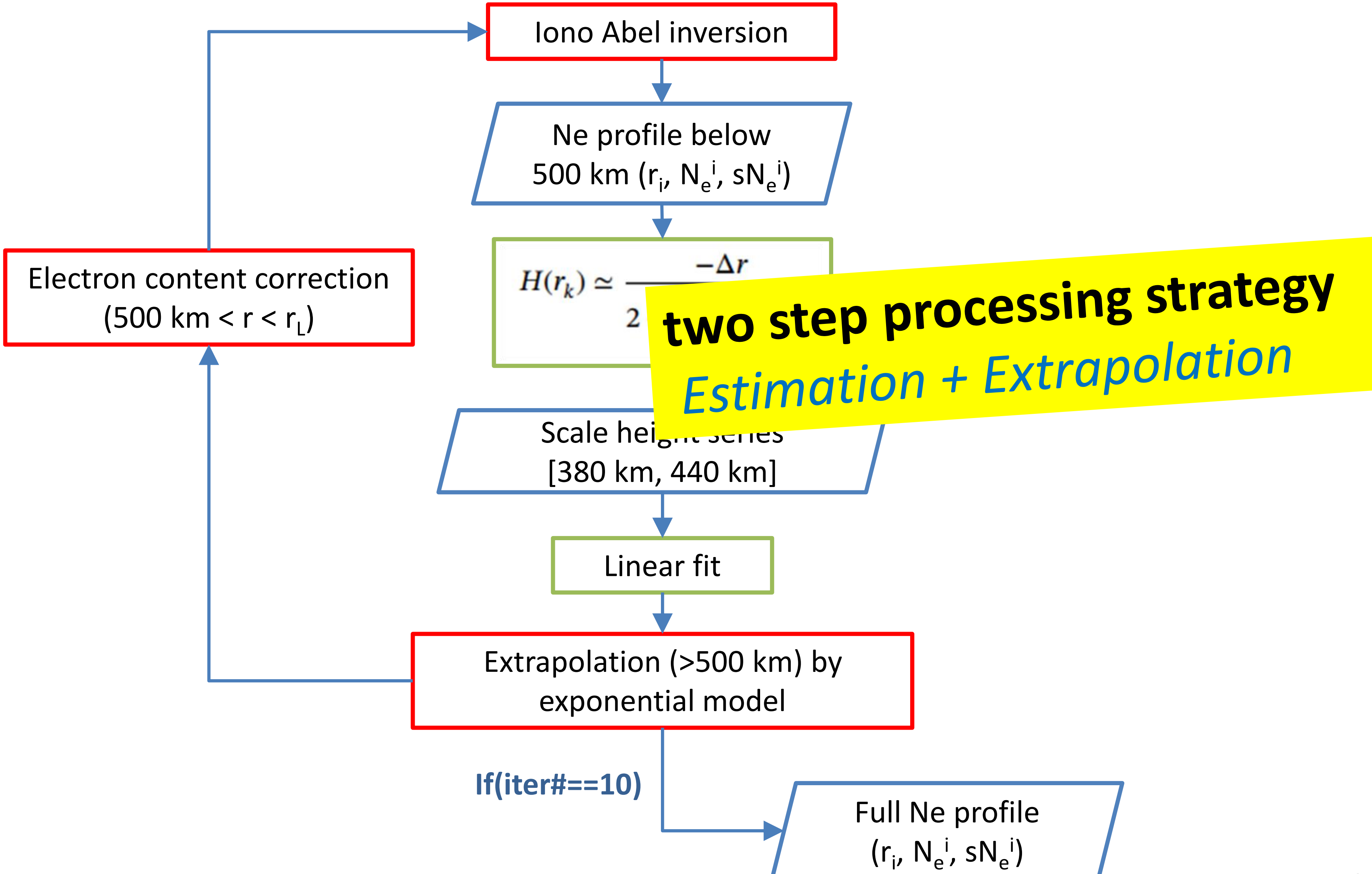

3. Method 2: AVHIRO

the Abel-VaryChap Hybrid modeling from topside Incomplete RO data

Estimate all the unknown parameters simultaneously

3. Method 2: AVHIRO

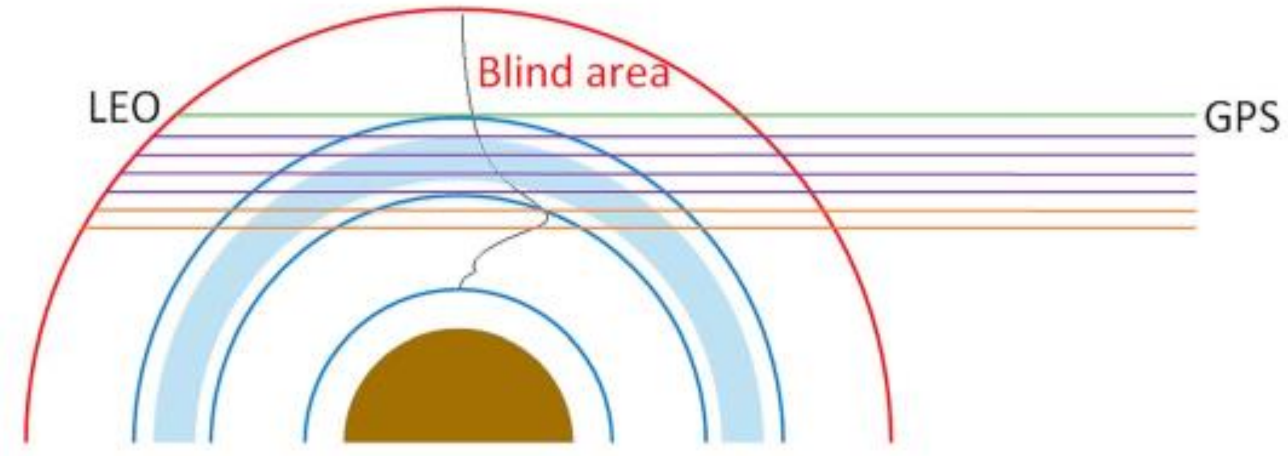

Observation equations (Ax=b): from top to bottom

$$
\begin{aligned}
(L_I)_1 &= \alpha\left(2l_{1,1}N_1 + 2l_{1,2}N_2 + \ \ldots\ + 2l_{1,x}N_x\right) + B_I \\
(L_I)_2 &= \alpha\left(2l_{2,1}N_1 + 2l_{2,2}N_2 + \ \ldots\ + 2l_{2,x}N_x + 2l_{2,x+1}N_{x+1}\right) + B_I \\
(L_I)_3 &= \alpha\left(2l_{3,1}N_1 + 2l_{3,2}N_2 + \ \ldots\ + 2l_{3,x}N_x + 2l_{3,x+1}N_{x+1}\right) + B_I \\
&\ldots \\
(L_I)_6 &= \alpha\left(2l_{6,1}N_1 + 2l_{6,2}N_2 + \ \ldots\ + 2l_{6,x}N_x + 2l_{6,x+1}N_{x+1} + 2l_{6,x+2}N_{x+2}\right) + B_I \\
&\ldots.
\end{aligned}
$$

L_I: the ionospheric combination of carrier phases

N_i: electron density in each layer

B_I: the corresponding ambiguity term

3. Method 2: AVHIRO

Example of Design matrix: $A_{200x319}$

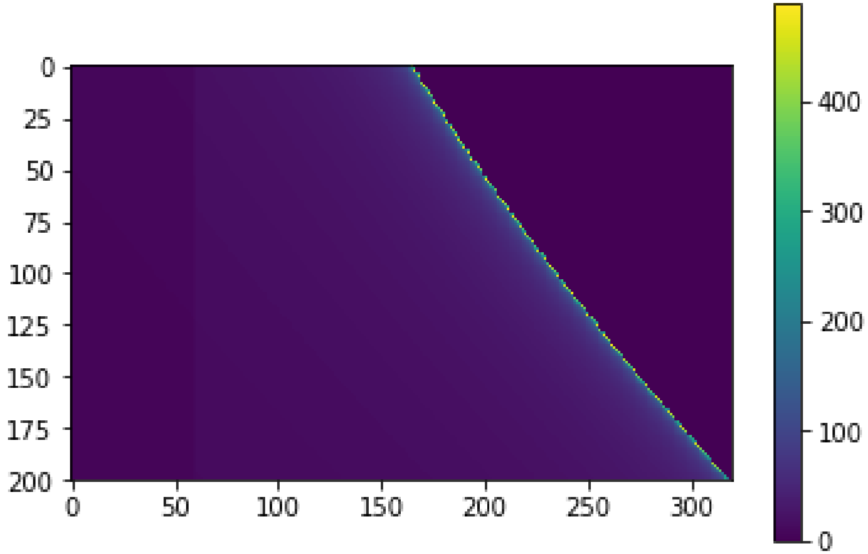

	0	1	2	...	317	318	319
0	16.657405	8.345719	8.368659	...	0.00000	0.00000	1.0
1	16.627440	8.330636	8.353439	...	0.00000	0.00000	1.0
2	16.597565	8.315598	8.338266	...	0.00000	0.00000	1.0
3	16.567779	8.300606	8.323138	...	0.00000	0.00000	1.0
4	16.538082	8.285658	8.308056	...	0.00000	0.00000	1.0
5	16.508473	8.270756	8.293021	...	0.00000	0.00000	1.0
6	16.478954	8.255899	8.278031	...	0.00000	0.00000	1.0
7	16.449524	8.241087	8.263088	...	0.00000	0.00000	1.0
8	16.420182	8.226320	8.248190	...	0.00000	0.00000	1.0
9	16.390929	8.211597	8.233338	...	0.00000	0.00000	1.0
10	16.361764	8.196920	8.218532	...	0.00000	0.00000	1.0
11	16.332687	8.182287	8.203772	...	0.00000	0.00000	1.0
12	16.303699	8.167700	8.189057	...	0.00000	0.00000	1.0

Layer thickness = ~3km

Ax=b: 1) rank deficient equations

2) ill-conditioned equations (column vectors of A matrix are highly related)

3. Method 2: AVHIRO

The unknown vector *x* in equation *Ax* = *b* is composed to three parts x^1(electron densities from 380 km to 1000 km), x^2 (electron densities below 380 km) and x^{ambi}

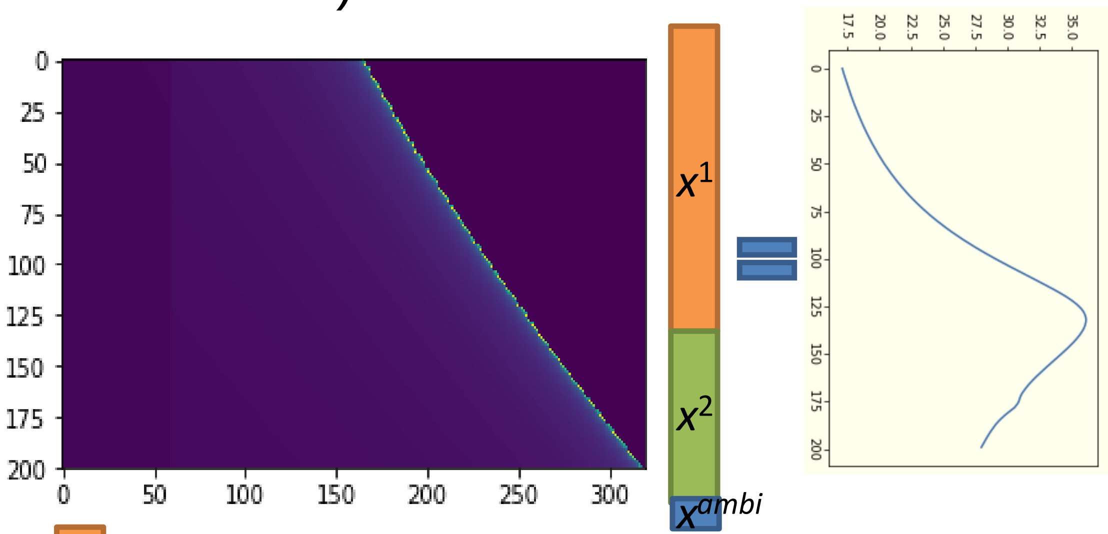

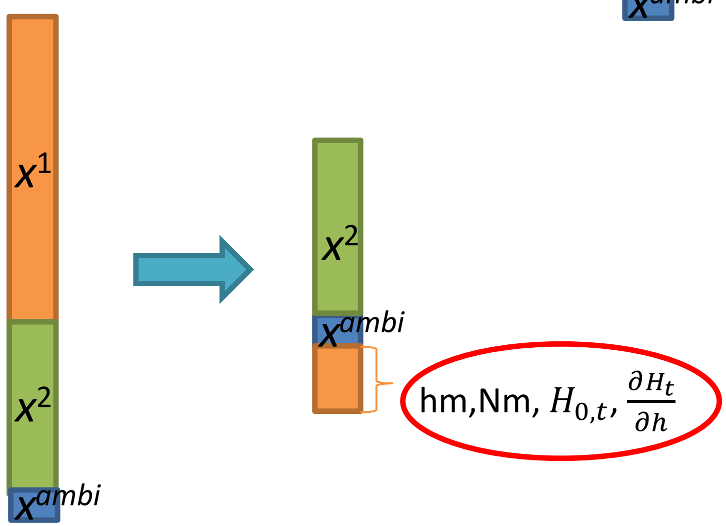

$$N = N_m e^{k(1-z-e^{-z})}, where\ z = \frac{h-hm}{H}$$

$$H_t(h) = \frac{\partial H_t}{\partial h}(h - h_m) + H_{0,t}\ ,\ h \geq h_m$$

3. Method 2: AVHIRO

The unknown vector x in equation $Ax = b$ is composed to three parts x^1(electron densities from 380 km to 1000 km), x^2 (electron densities below 380 km) and x^{ambi}

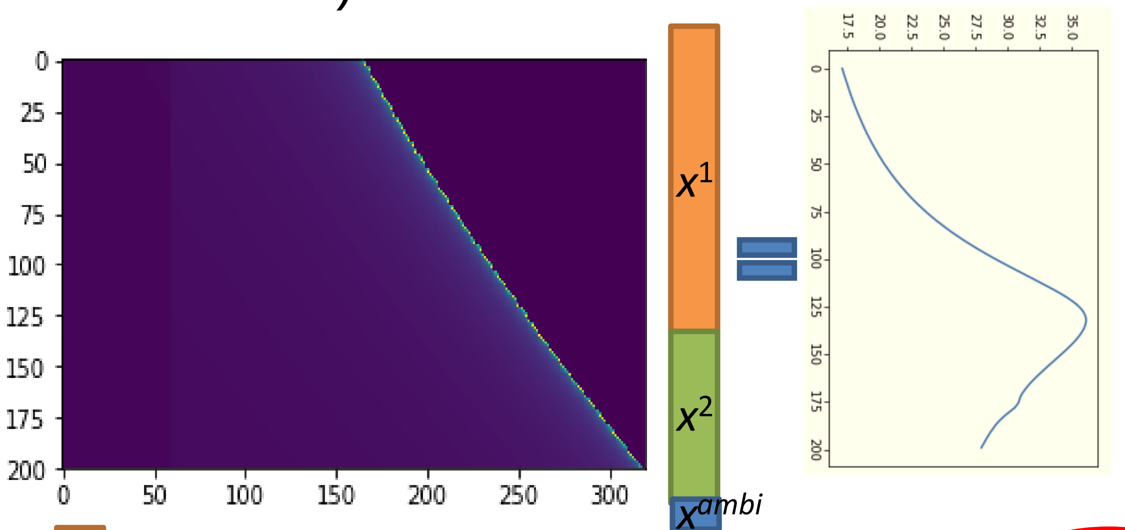

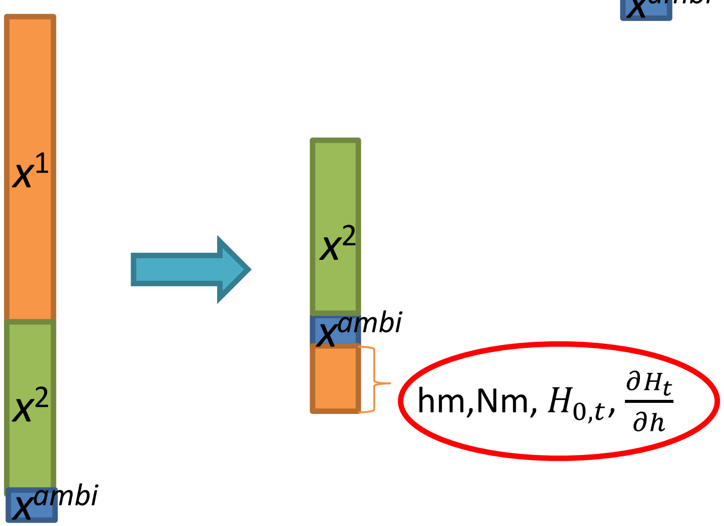

$$N = N_m e^{k(1-z-e^{-z})} \quad where\ z = \frac{h-hm}{H}$$

$$H_t(h) = \frac{\partial H_t}{\partial h}(h - h_m) + H_{0,t}\ ,\ h \geq h_m$$

Nonlinear: two exponential terms

3. Method 2: AVHIRO

The unknown vector x in equation $Ax = b$ is composed to three parts x^1(electron densities from 380 km to 1000 km), x^2 (electron densities below 380 km) and x^{ambi}

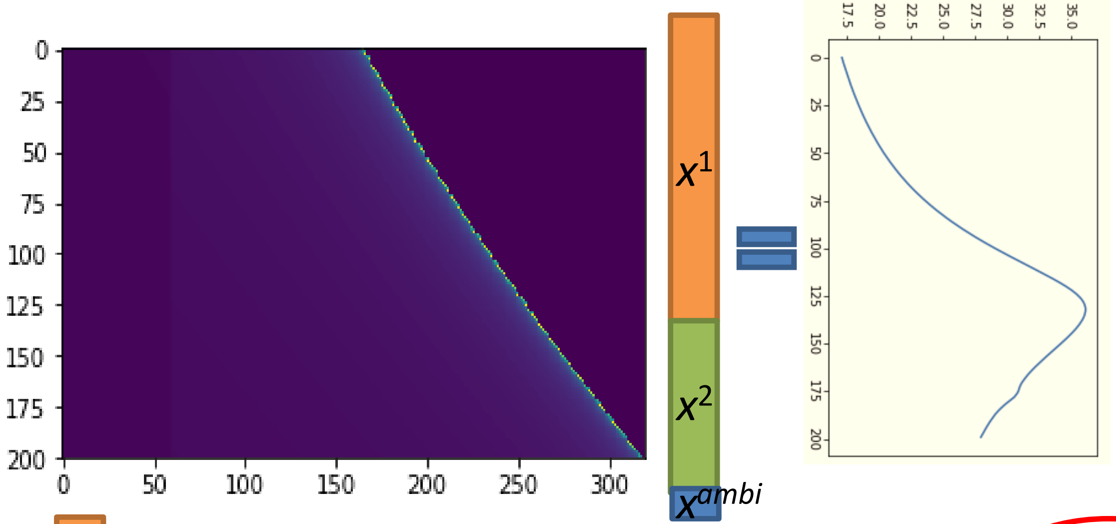

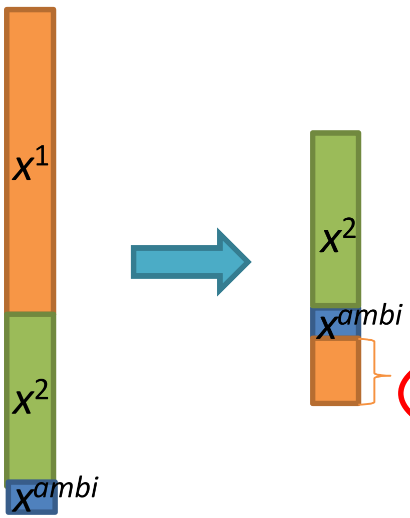

hm,Nm, $H_{0,t}$, $\frac{\partial H_t}{\partial h}$

$$N = N_m e^{k(1-z-e^{-z})} \quad where\ z = \frac{h-hm}{H}$$

$$H_t(h) = \frac{\partial H_t}{\partial h}(h - h_m) + H_{0,t}\ ,\ h \geq h_m$$

Nonlinear: two exponential terms

Linearization

3. Method 2: AVHIRO

The unknown vector x in equation $Ax = b$ is composed to three parts x^1(electron densities from 380 km to 1000 km), x^2 (electron densities below 380 km) and x^{ambi}

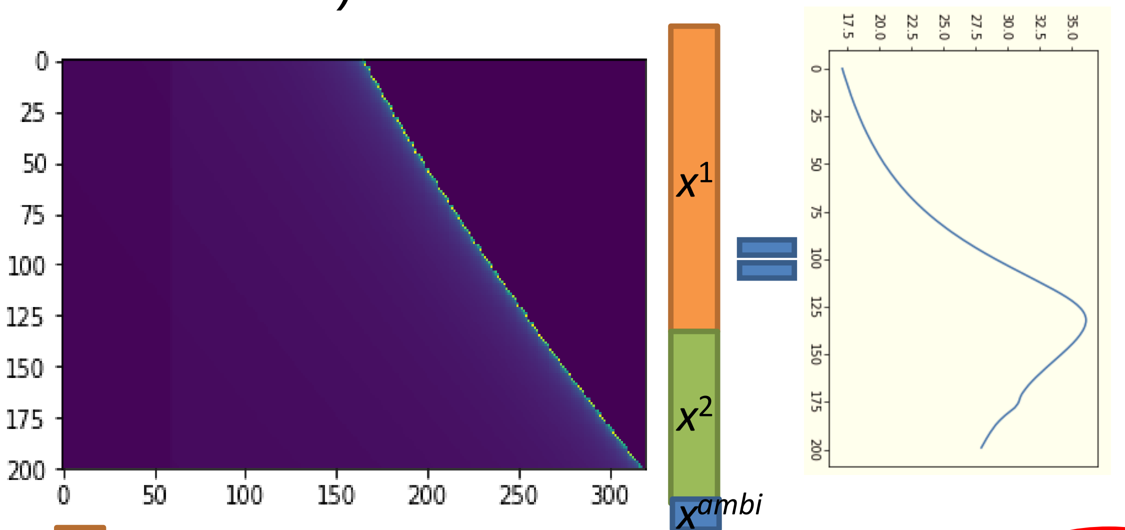

$$N = N_m e^{k(1-z-e^{-z})} \quad where\ z = \frac{h - hm}{H}$$

$$H_t(h) = \frac{\partial H_t}{\partial h}(h - h_m) + H_{0,t}\ ,\ h \geq h_m$$

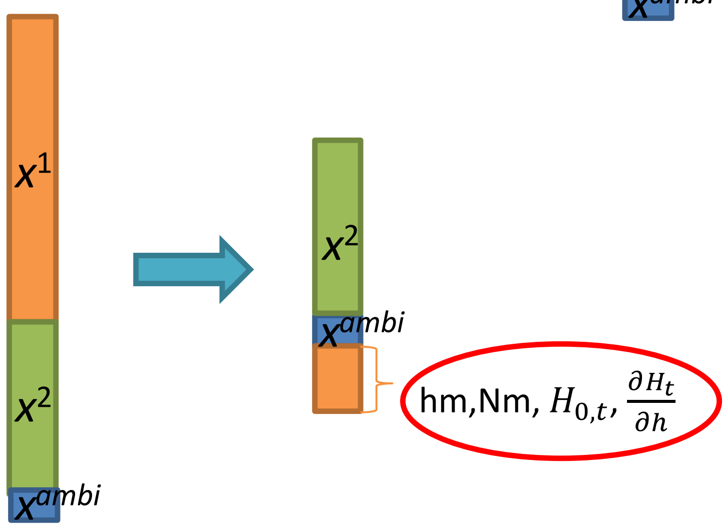

Nonlinear: two exponential terms

~~*Linearization*~~

3. Method 2: AVHIRO

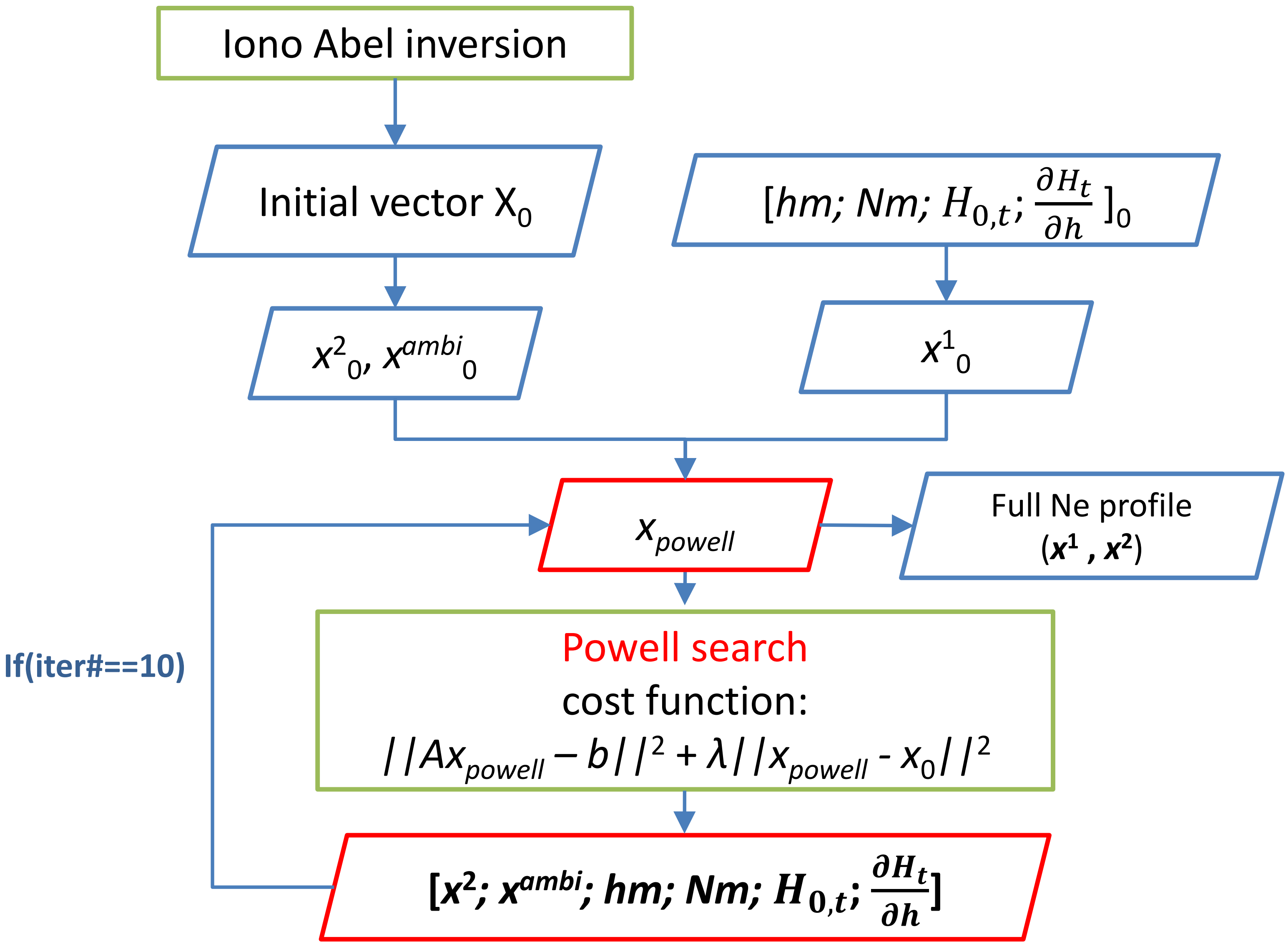

3. Method 2: AVHIRO

solve **the full electron densities** (up to 1000 km), **ambiguity term** and **four parameters of Vary-Chap model** simultaneously.

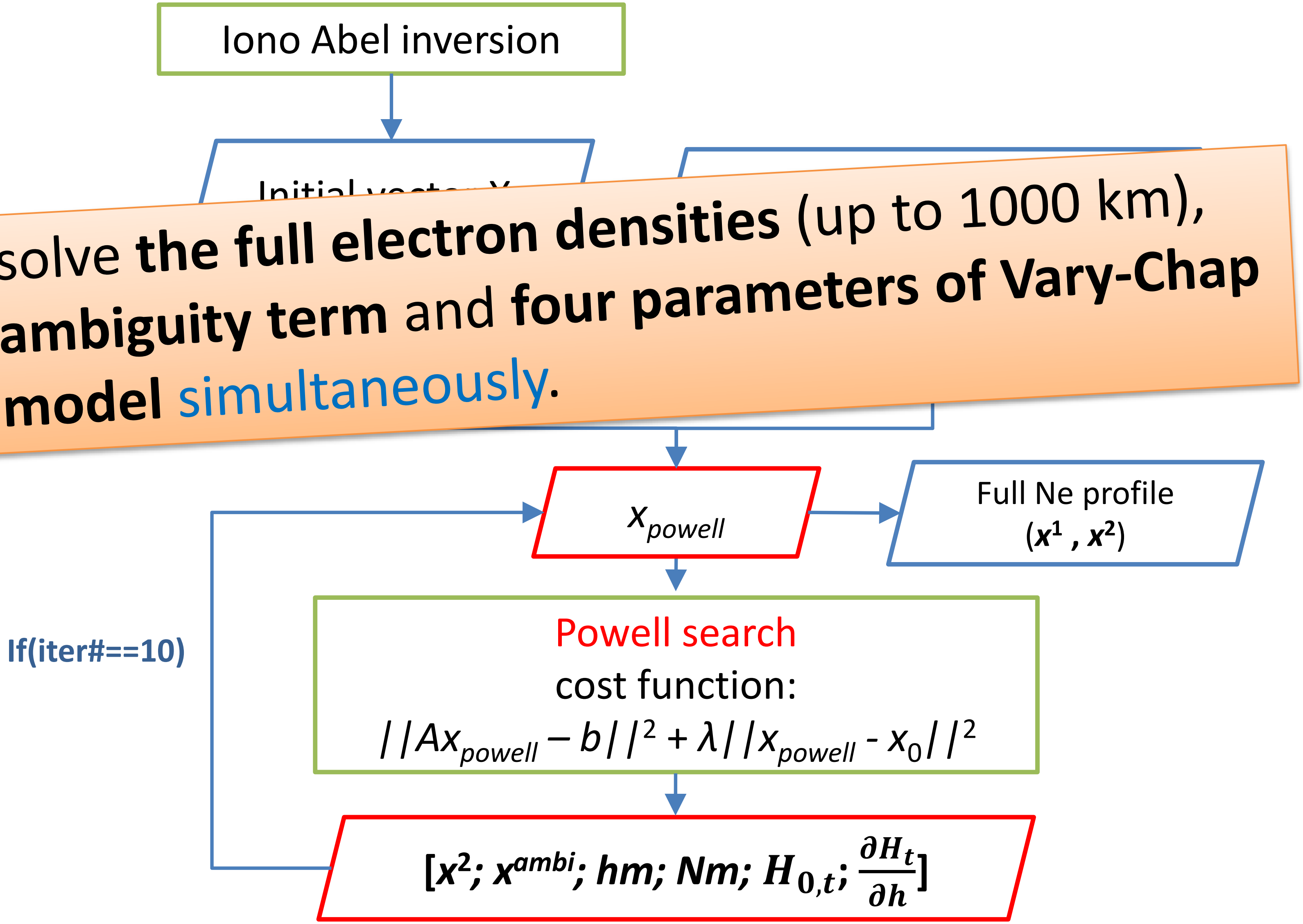

4. Assessment

4.1 SEEIRO assessment (<500km)

4.2 AVHIRO assessment (<500km)

4.3 Other aspects of assessment regarding AVHIRO

Representative scenarios of major storm, solar cycle minimum and maximum conditions: +3700 COSMIC/FORMOSAT3 radio-occultations (inverted in terms of electron density profiles with improved Abel inversion)

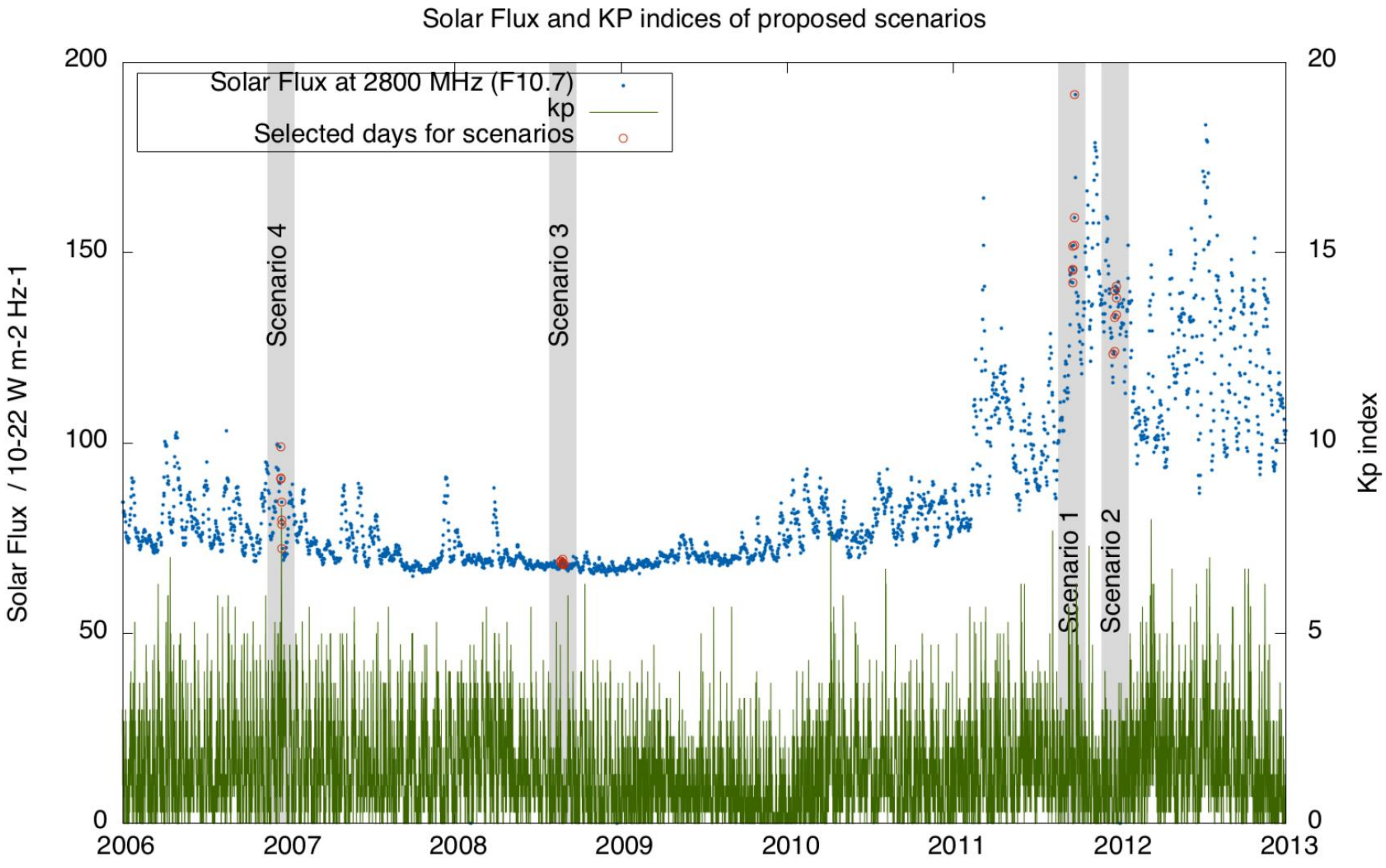

Example for a typical single RO
day 261, 2011, ~37323sec, PRN13, rec.l220 (arc#6)

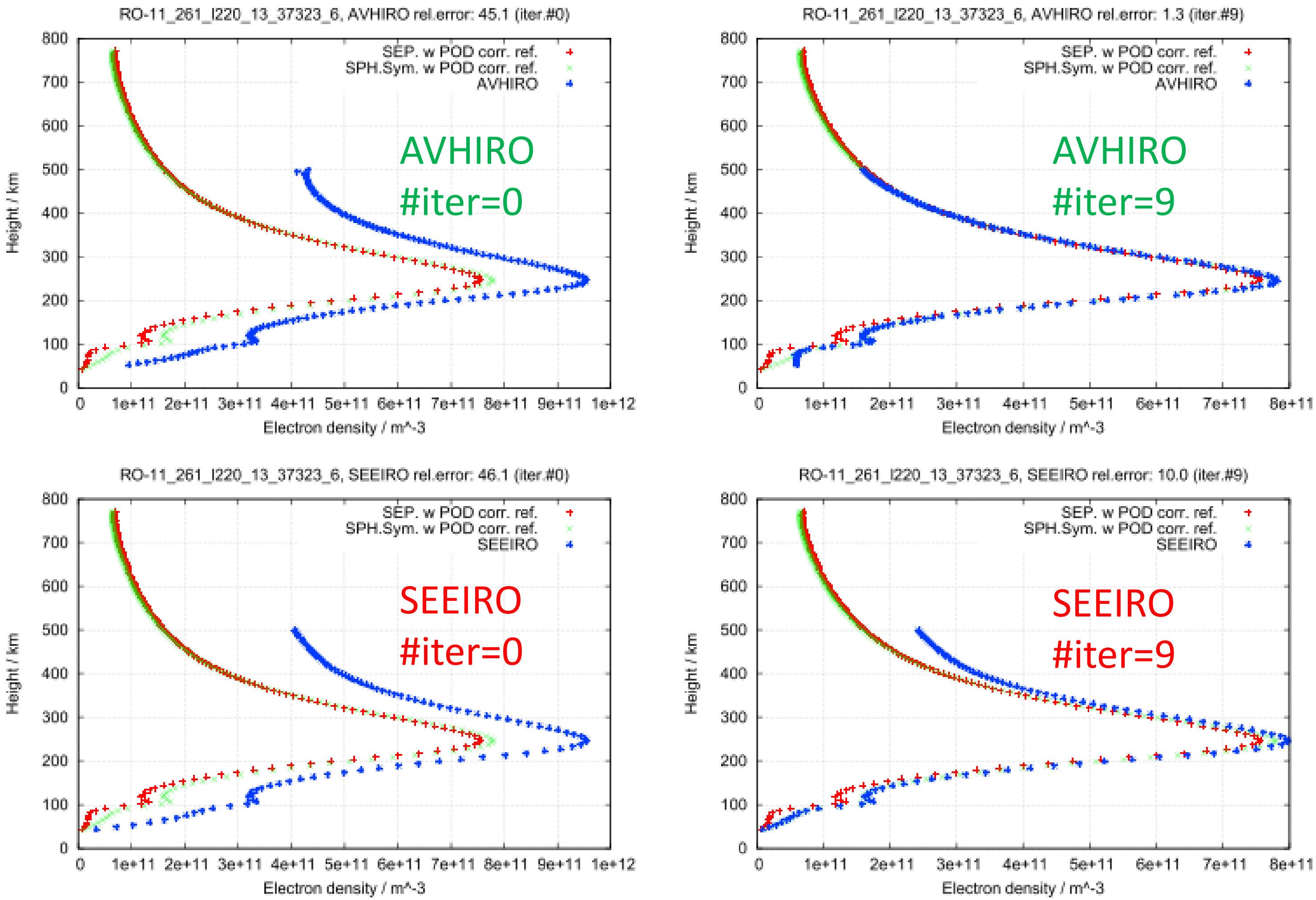

Ref 1: Abel inversion modeling the horizontal variabilty with separability concept from complete RO data

Ref 2: Abel inversion under assumption of spherical symmetry from complete RO data

4.1 SEEIRO assessment (<500km)

4.1 SEEIRO assessment (<500km)

Distribution of absolute errors (28-days representative data)

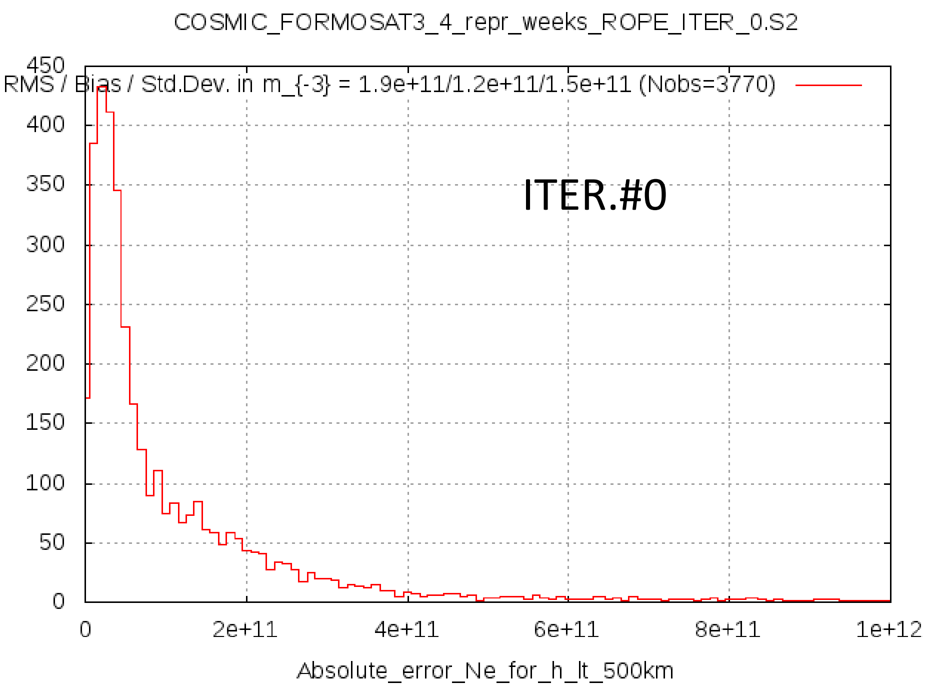

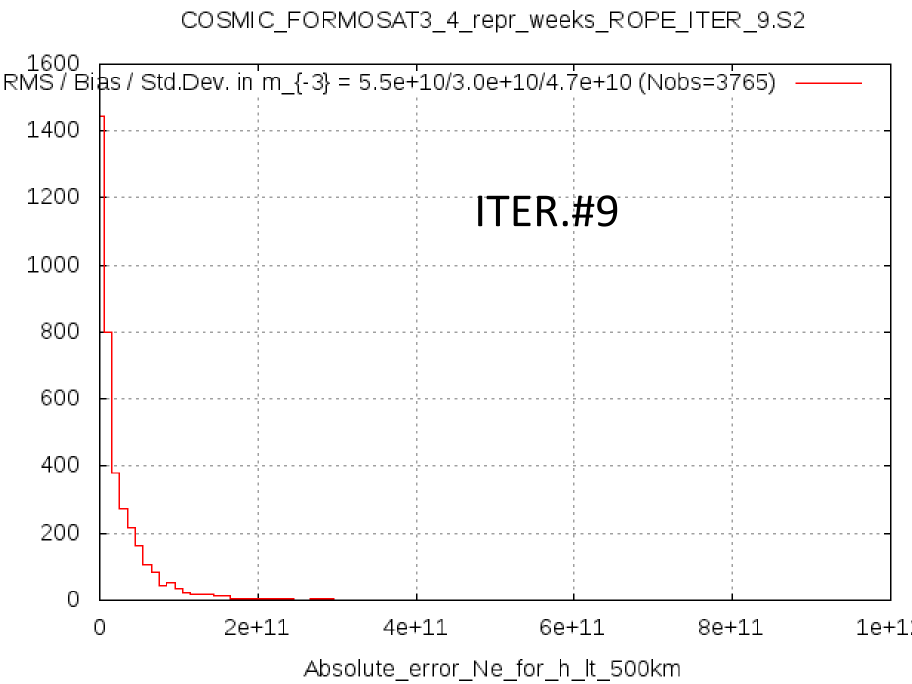

Abs.Error BEFORE SEEIRO:
1.2e+11 m^{-3} +/- 1.5e+11 m^{-3}

Abs.Error AFTER SEEIRO:
3.0e+10 m^{-3}+/- 4.7e+10 m^{-3}

4.1 SEEIRO assessment (<500km)

Distribution of relative errors (28-days representative data)

Each profile:

$$Rel.err = \frac{RMS(\Delta Ne)}{RMS(Ne\_ref)} \times 100\%$$

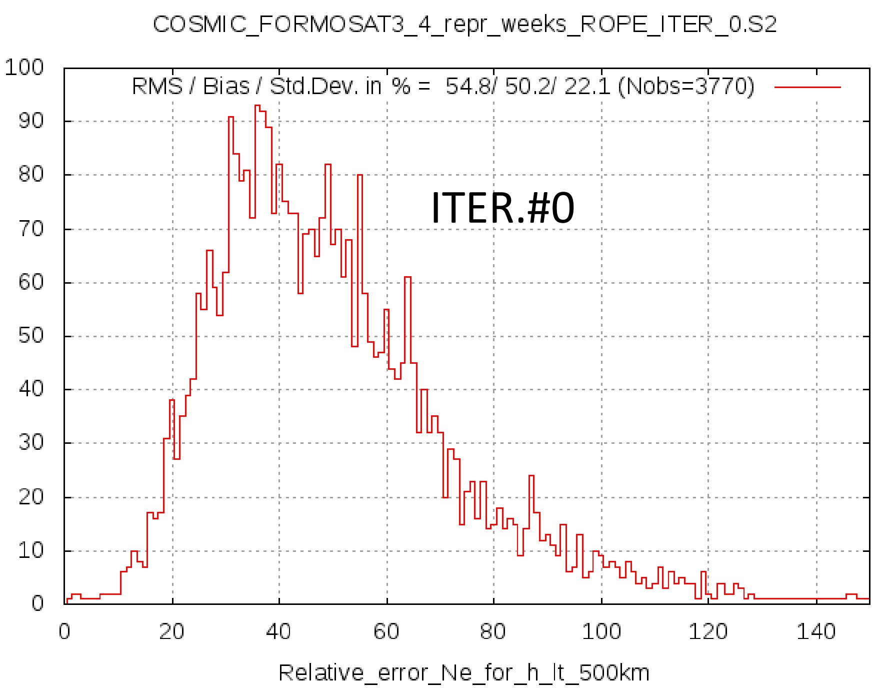

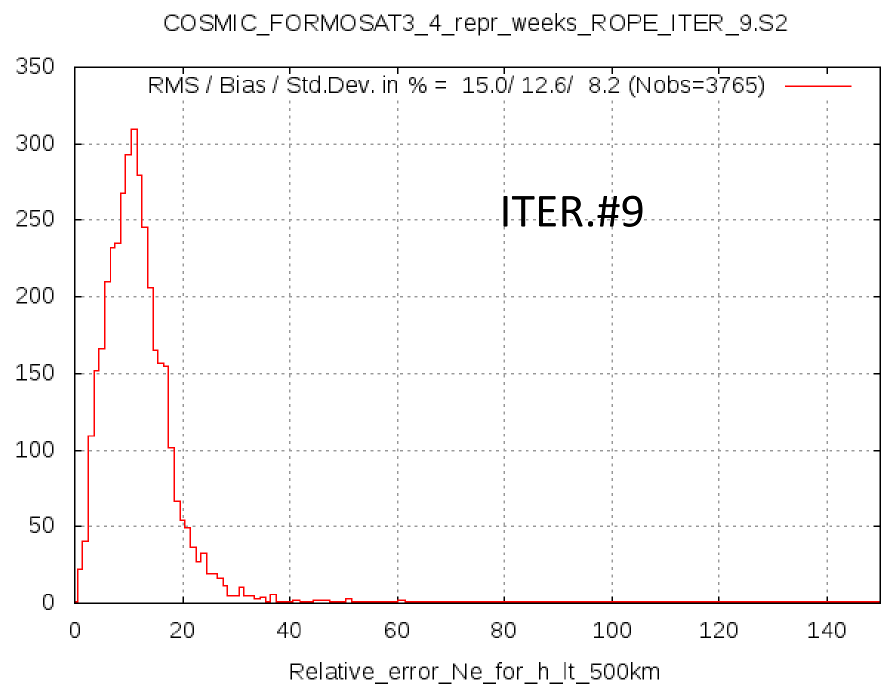

Rel.Error BEFORE SEEIRO:
50% +/- 22%

Rel.Error AFTER SEEIRO:
13% +/- 8%

4.2 AVHIRO assessment (<500km)

4.2 AVHIRO assessment (<500km)

Distribution of absolute errors (28-days representative data)

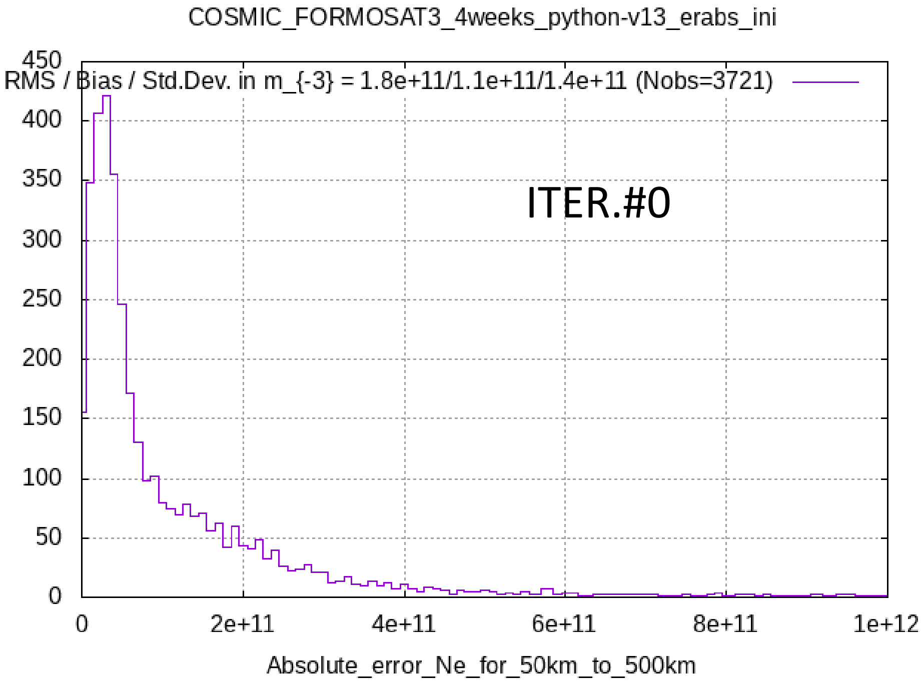

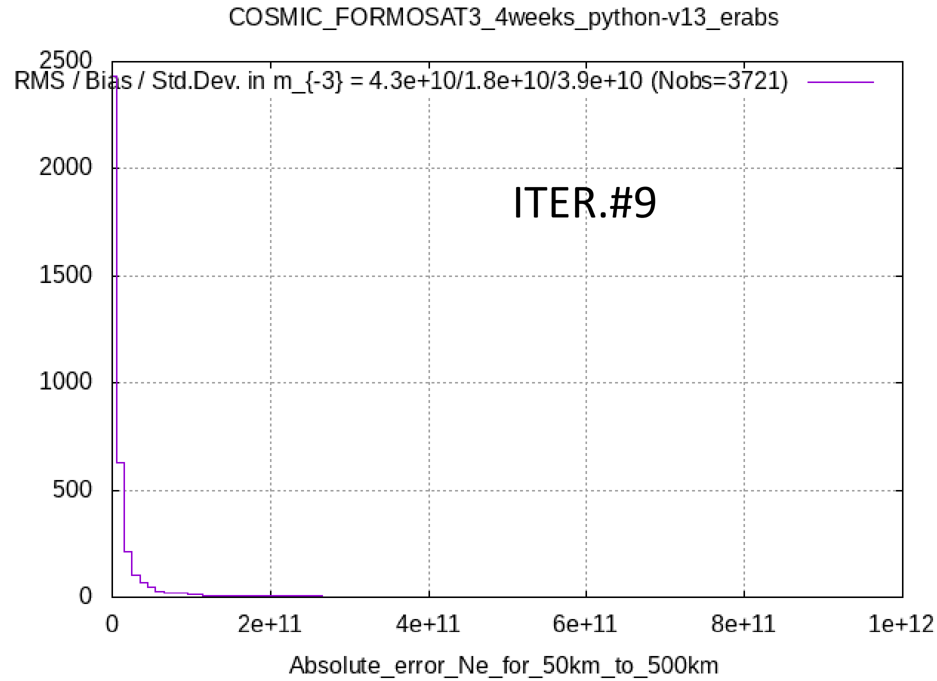

Abs.Error BEFORE AVHIRO:
1.1e+11 m^{-3} +/- 1.4e+11 m^{-3}

Abs.Error AFTER AVHIRO:
1.8e+10 m^{-3}+/- 3.9e+10 m^{-3}

4.2 AVHIRO assessment (<500km)

Distribution of relative errors (28-days representative data)

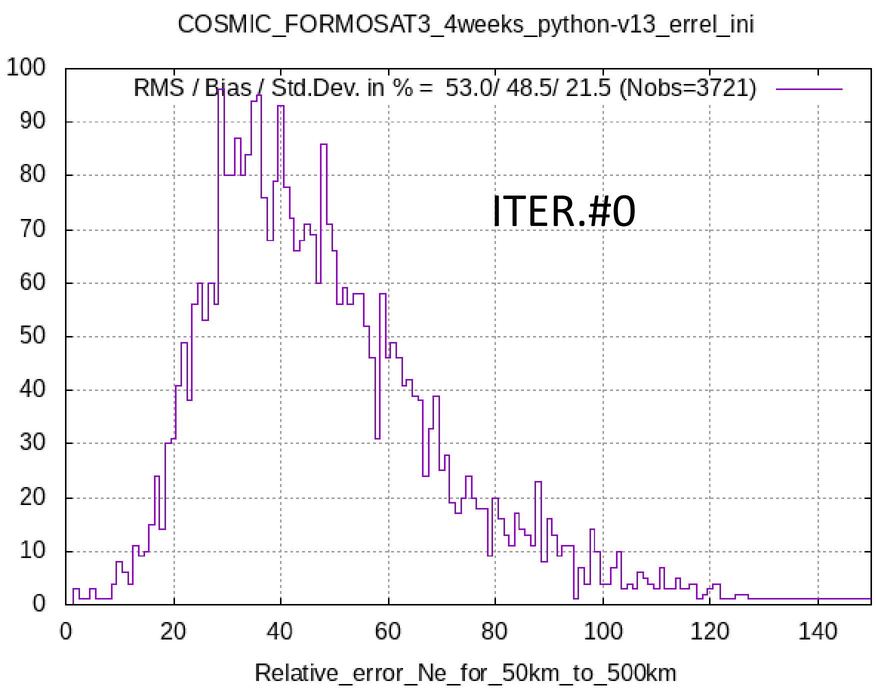

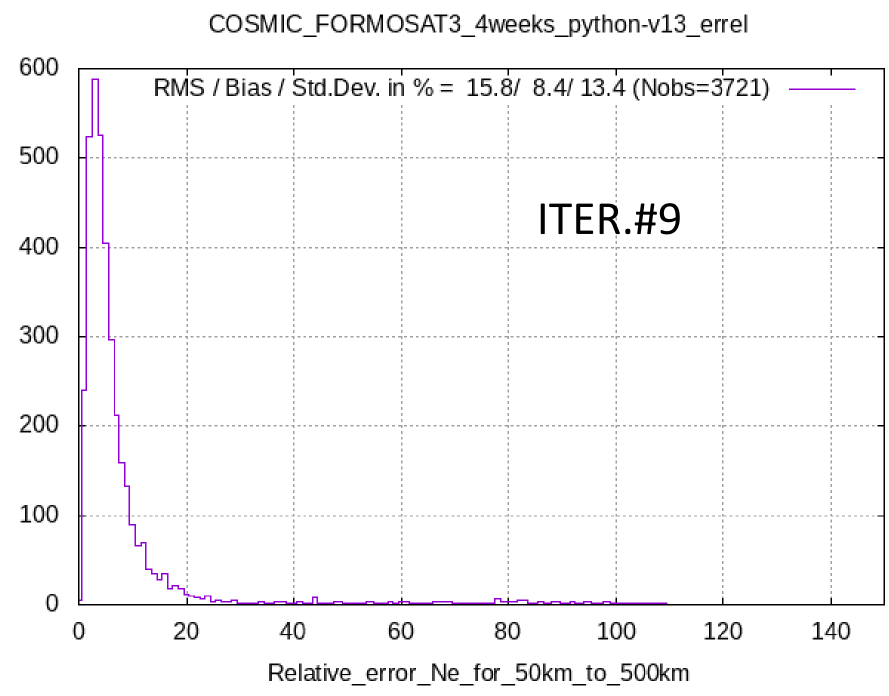

Rel.Error BEFORE AVHIRO: 49% +/- 22%

Rel.Error AFTER AVHIRO: 8% +/- 13%

4.2 AVHIRO assessment (<500km)

Distribution of relative errors (28-days representative data)

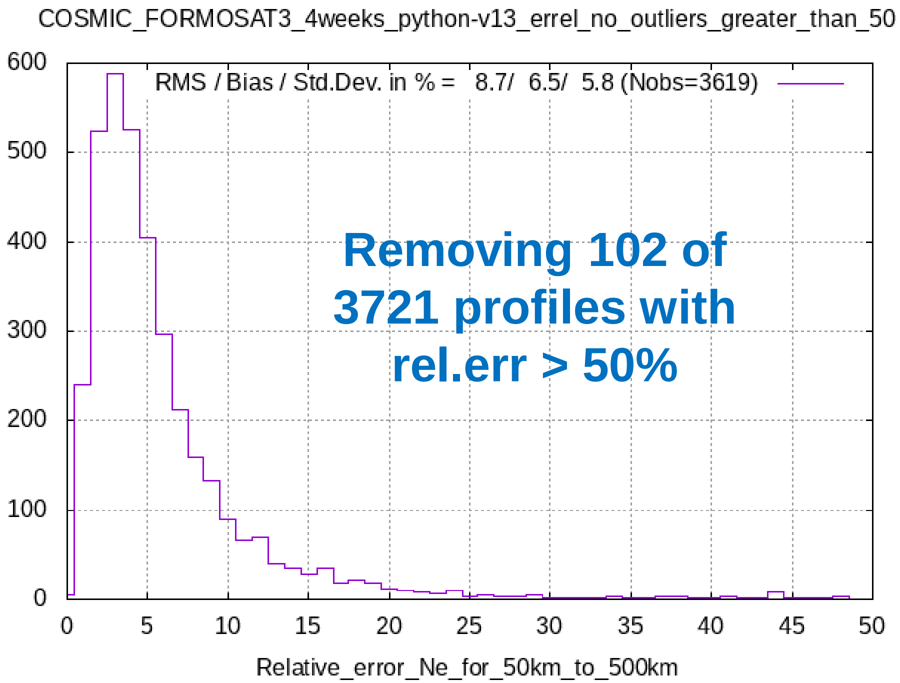

Rel.Error AFTER AVHIRO:
7% +/- 6%

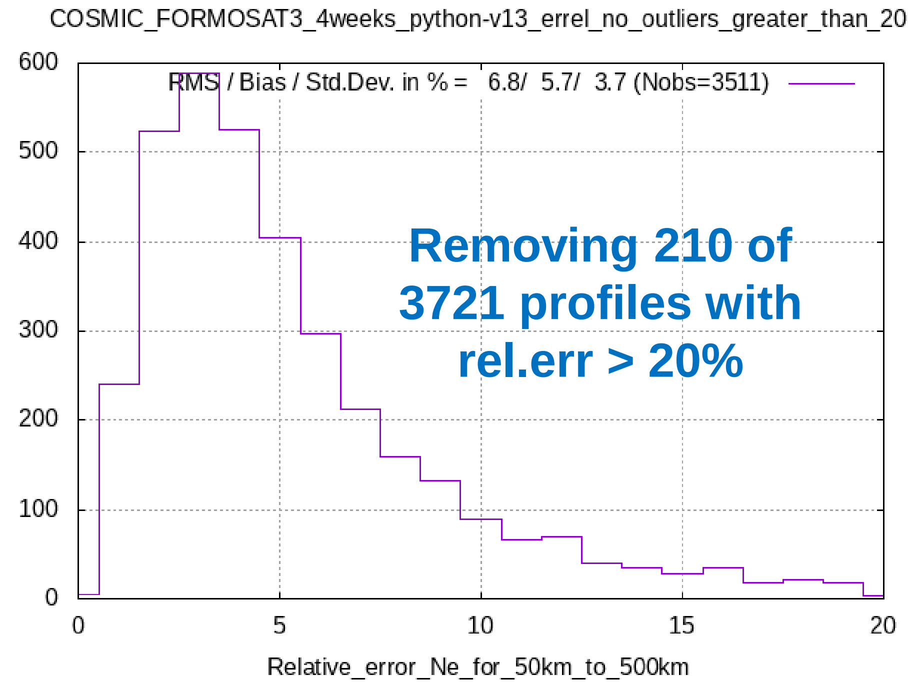

Rel.Error AFTER AVHIRO:
6% +/- 4%

4.3 Other aspects of assessment regarding AVHIRO

Absolute error below and above 500 km

Below 500 km

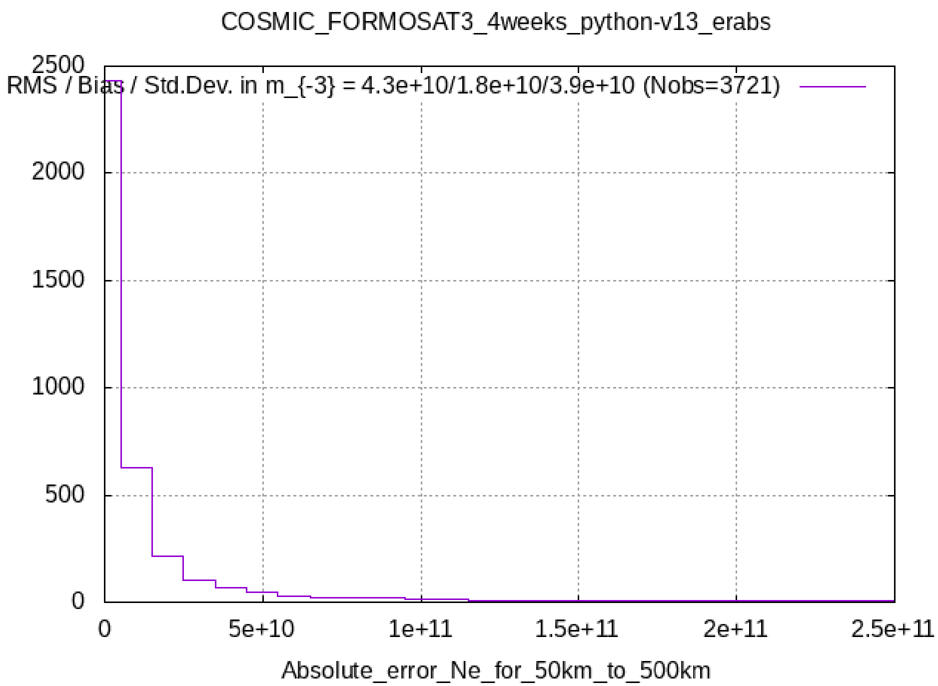

Abs.Error:

$1.8e+10\ m^{-3}$ +/- $3.9e+10\ m^{-3}$

Blind area: above 500 km

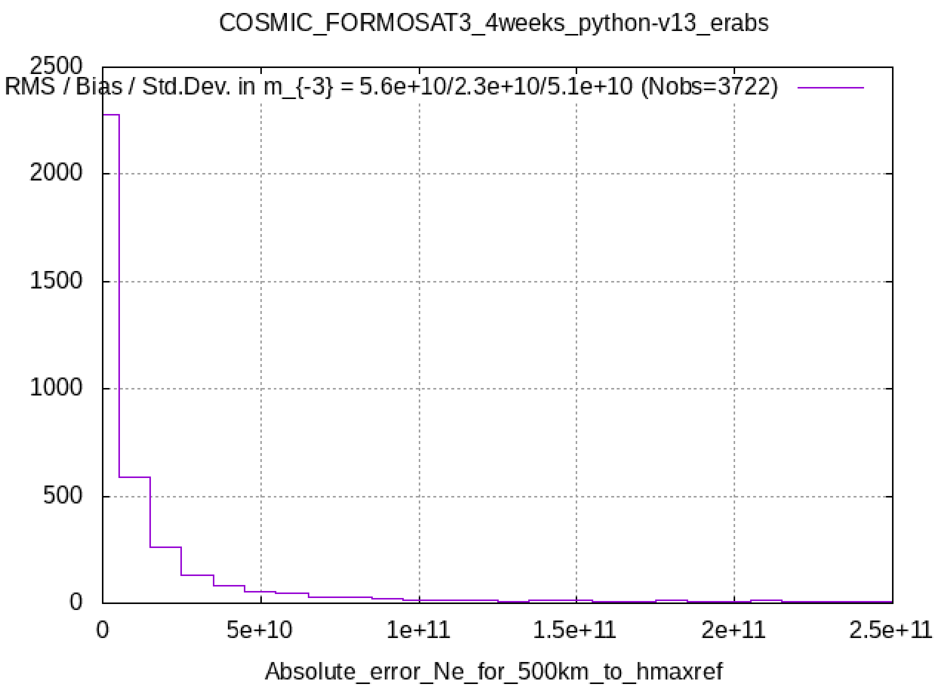

Abs.Error:

$2.3e+10\ m^{-3}$ +/- $5.1e+10\ m^{-3}$

Relative error below and above 500 km

$$\text{Each profile: Rel.err} = \frac{RMS(\Delta Ne)}{RMS(Ne\_ref)} \times 100\%$$

Below 500 km

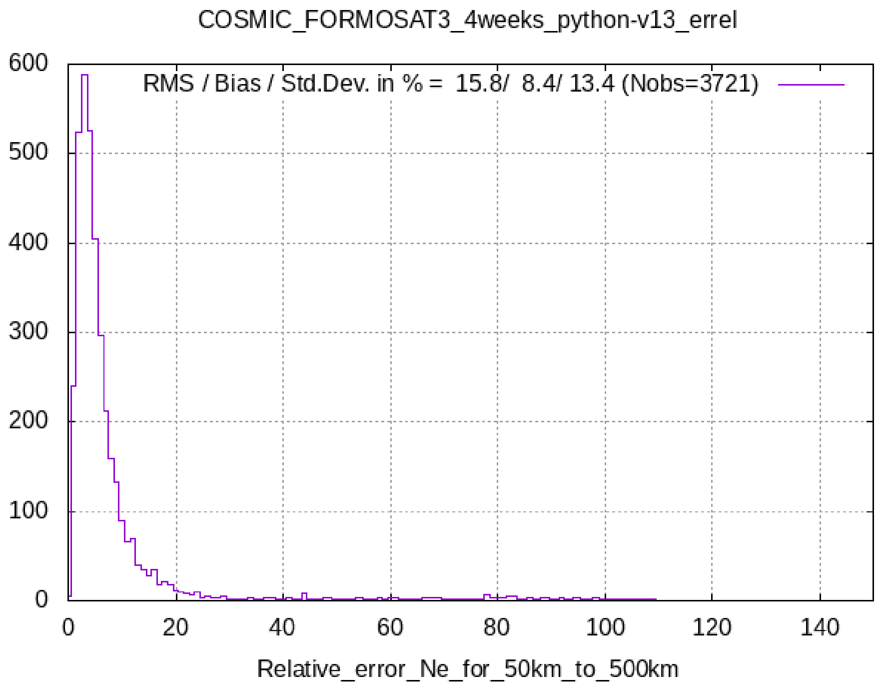

Rel.Error:

8% +/- 13%

Blind area: above 500 km

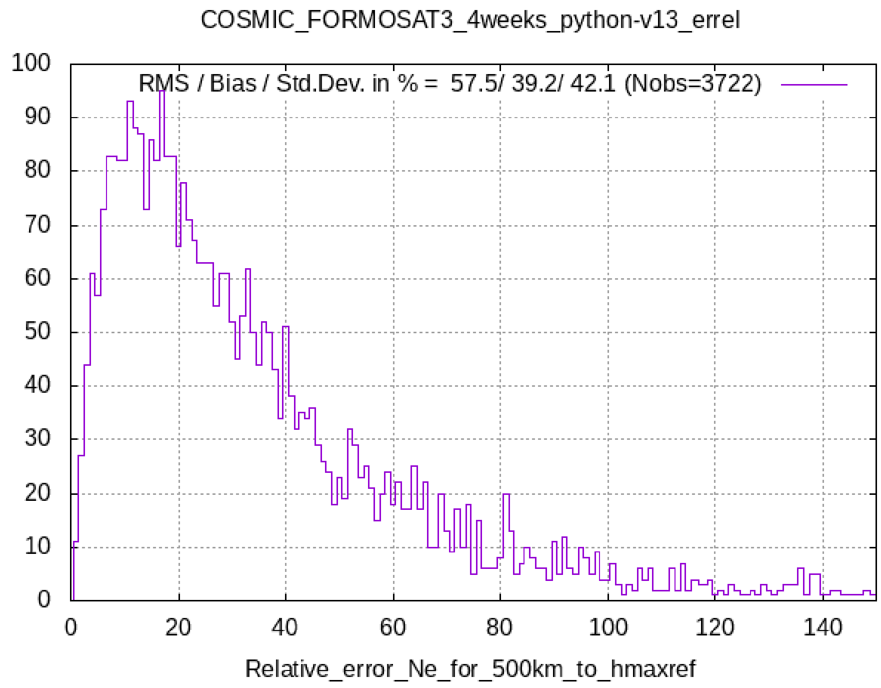

Rel.Error:

39% +/- 42%

Four examples of precision above 500 km

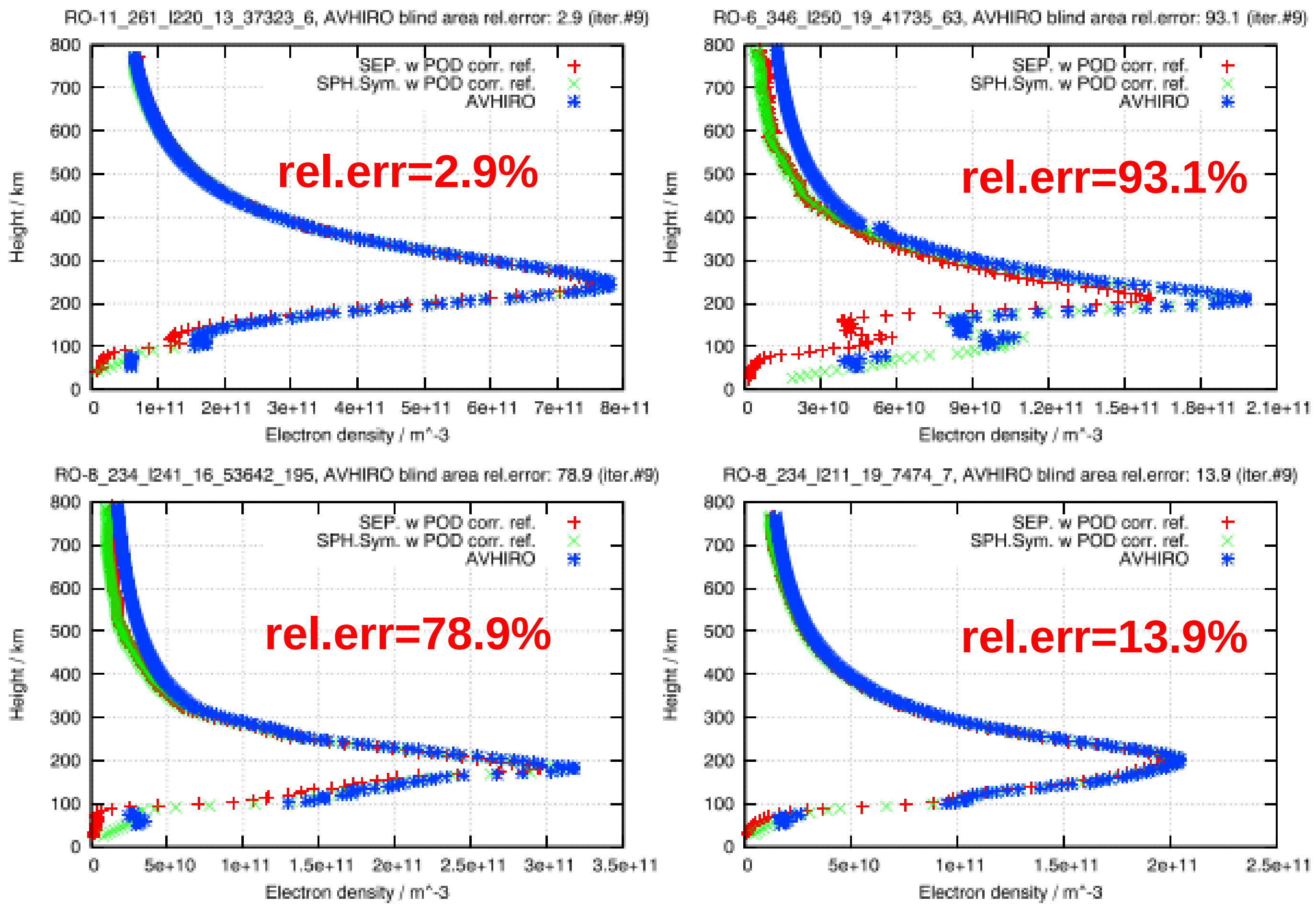

Ref 1: Abel inversion modeling the horizontal variabilty with separability concept from complete RO data

Ref 2: Abel inversion under assumption of spherical symmetry from complete RO data

AVHIRO: Abel-VaryChap Hybrid density profile from topside Incomplete RO data

Absolute Error vs. height

ITER.#0

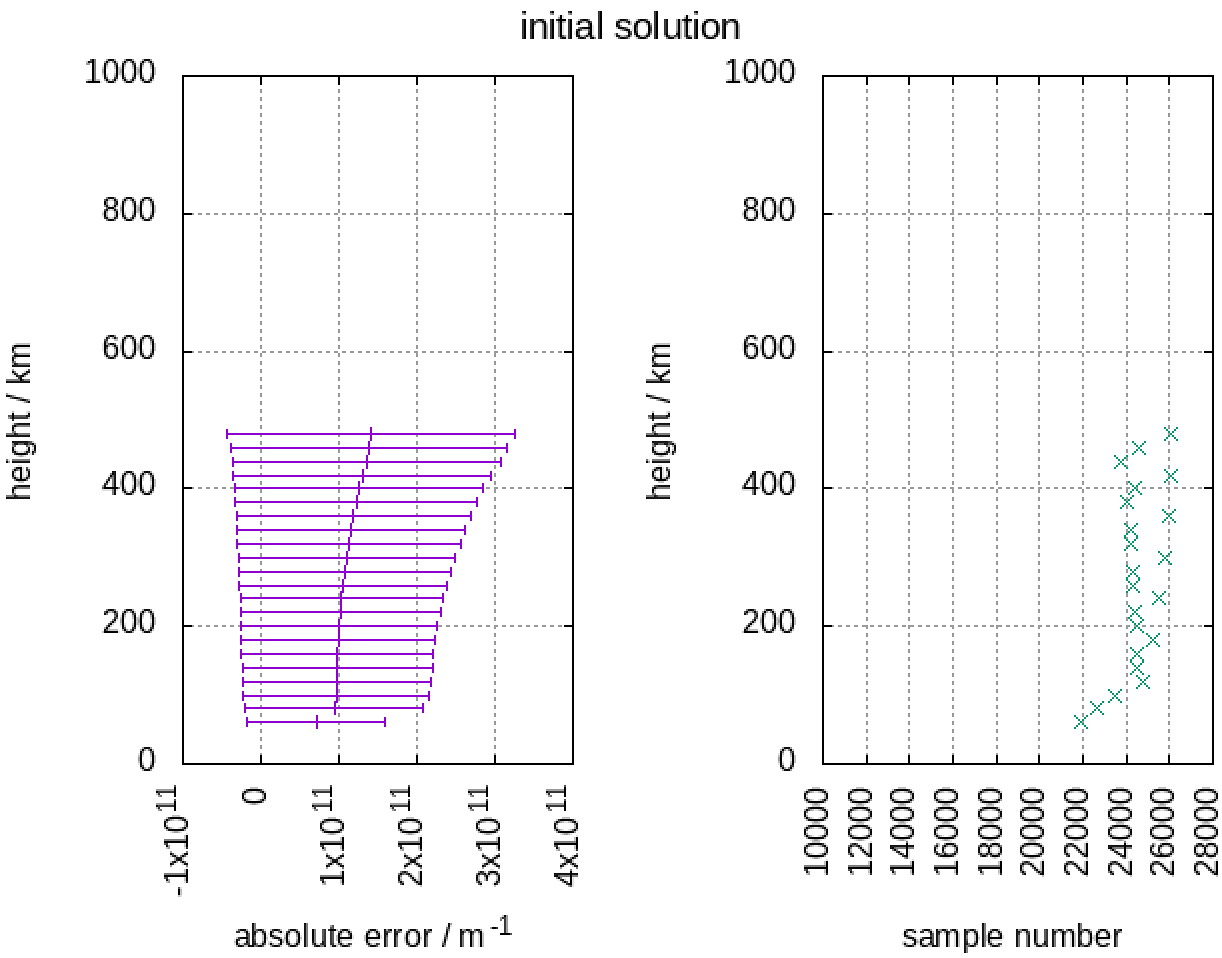

Absolute Error vs. height

ITER.#9

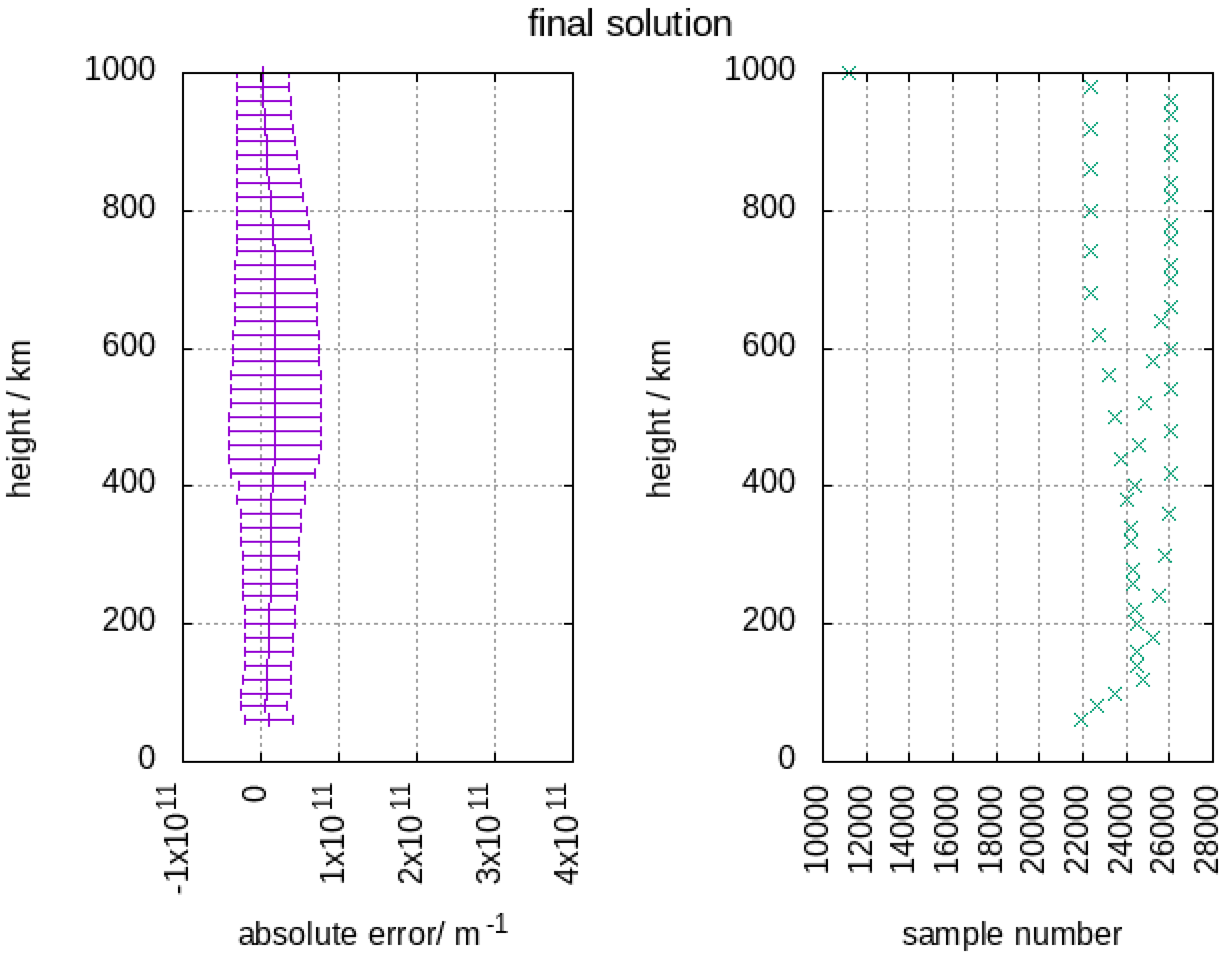

Pros and Cons: Summary

	AVHIRO	SEEIRO
Ne Relative Accuracy	**8%**	13%
Predominant Ne Rel. Acc.	**3%**	10%
Ne Absolute Accuracy	**$(1.8\times10^{10}$ +/- $3.9\times10^{10})m^{-3}$**	$(3.0\times10^{10}$ +/- $4.7\times10^{10})$ m^{-3}
Predominant Ne Abs. Acc.	<**$10^{10}m^{-3}$**	<**$10^{10}m^{-3}$**
CPU time per preprocessed RO	20 minutes **(~2min in future parallel version)**	**17 seconds**
Suitable for NRT service?	No	**Yes**
Suitable for PP service?	**Yes**	Backup option for PP
Required ancillary information?	**No**	**No**
Required inputs	Dual-frequency GPS carrier phase measurements, predicted GPS and LEO orbits	
Convenient inputs	Dual-frequency GPS POD carrier phase meas.	

5. Conclusions (1/2)

1. In this work, two methods - SEEIRO and AVHIRO - are presented as new techniques to retrieve full electron density profile from truncated RO data, without the need of external data.
2. SEEIRO reduces the relative error of the RO inversion with data up to 500 km regarding to the full data inversion up to 800 km, from *50% (+/-22%) before, to **13%(+/-8%)***
3. AVHIRO reduces the electron density error of the RO inversion with measurements up to 500 km regarding to the full inversion with observations up to 800 km: from *49% (+/-22%)* before to ***8%(+/-13%)***.
4. AVHIRO reduces the predominant relative error to 3% compared with the 10% obtained with the fast SEEIRO approach.

5. Conclusions (2/2)

5. AVHIRO provides simultaneously the linear Vary-Chapman extrapolated electron density profile with accuracy slightly lower than those obtained at heights below 500 km with observations: **$(2.3 \pm 5.1) \times 10^{10}$ m^{-3}** above versus **$(1.8 \pm 3.9) \times 10^{10}$ m^{-3}** below 500 km.

6. **SEEIRO** solves the problem by two step processing strategy and needs less computation time, suitable for **Near Real-Time** determination. **AVHIRO** estimates the full electron density profile simultaneously and achieves more accurate results, yet at higher computational cost, suited for **postprocessing**.

Remarks

In the proof of concept of SEEIRO and AVHIRO, spherical symmetry is assumed. The improved Abel inversion taking into account horizontal gradients will be easily applied in a straightforward way under separability hypothesis by substituting Ni = Vi * Si, where Vi is the VTEC at the corresponding "i" crossing point (given for instance by GIM) and being Si, the "shape function", the new unknown.

Reference

1. Olivares-Pulido, G., Hernández-Pajares, M., Aragón-Àngel, A., & García-Rigo, A. (2016). A linear scale height Chapman model supported by GNSS occultation measurements. *Journal of Geophysical Research: Space Physics*, *121*, 7932–7940. https://doi.org/10.1002/2016JA022337
2. Hernández-Pajares, M., Garcia-Fernàndez, M., Rius, A., Notarpietro, R., von Engeln, A., Olivares-Pulido, G., et al. (2017). Electron density extrapolation above F2 peak by the linear Vary-Chap model supporting new Global Navigation Satellite Systems-LEO occultation missions. *Journal of Geophysical Research: Space Physics*, *122*, 9003–9014. https://doi.org/10.1002/2017JA023876
3. Prol, F. d. S., Themens, D. R., Hernández-Pajares, M., Camargo, P. d. O., & Muella, M. T. d. A. H. (2019). Linear Vary-Chap topside electron density model with topside sounder and radio-occultation data. *Surveys in Geophysics*, *40*, 1–17. https://doi.org/10.1007/s10712-019-09521-3
4. Lyu, H., Hernández-Pajares, M., Monte-Moreno, E., & Cardellach, E. (2019). Electron density retrieval from truncated Radio Occultation GNSS data. *Journal of Geophysical Research: Space Physics, 124*(6), 4842-4851.

Thank you for your attention !

Backup 1

The Vary-Chapman Extrapolation Technique (VCET)

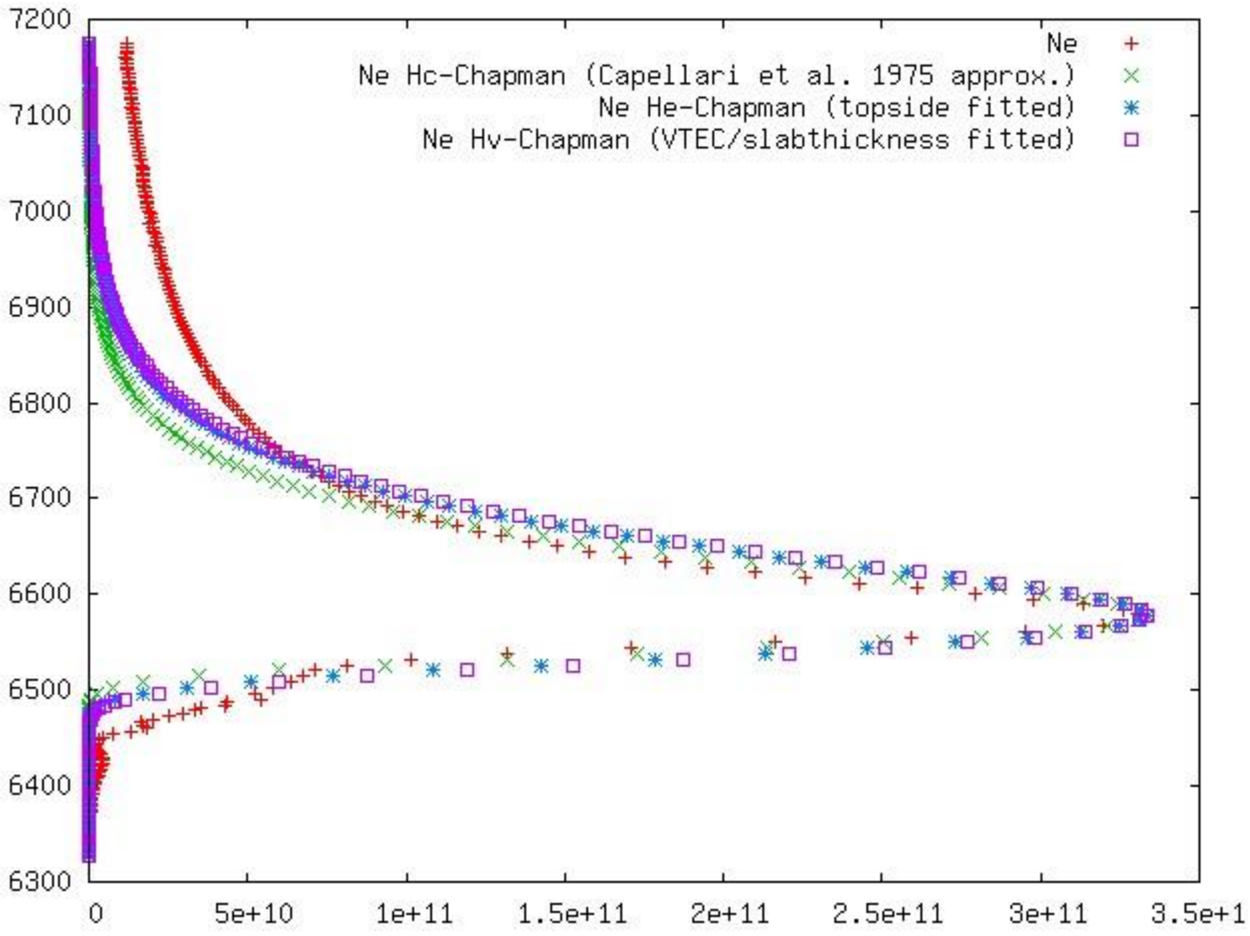

Backup 2

Summary of results on the +3700 occultations in the 4 scenarios

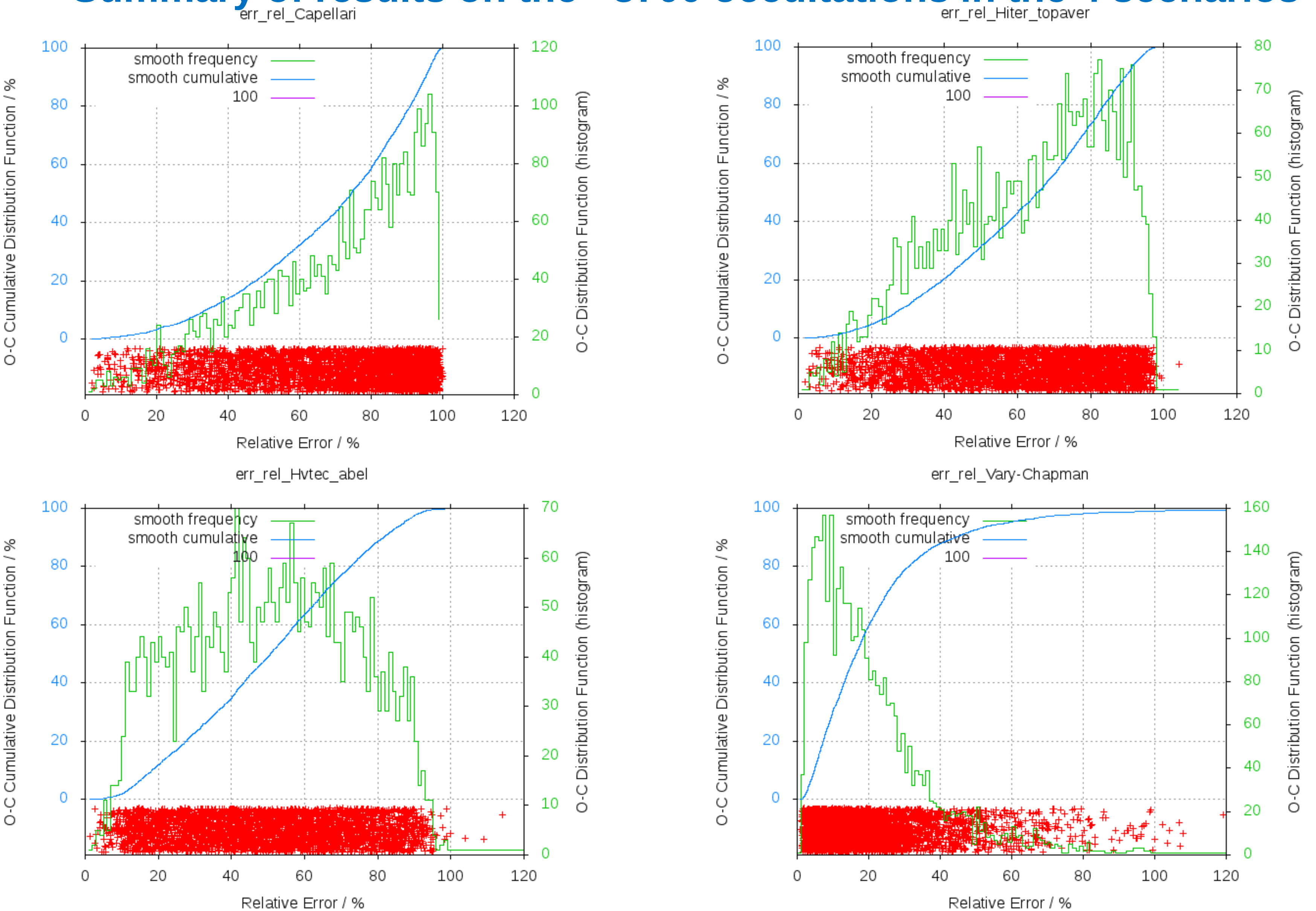

Backup 3

Convergence for ROs of a single day (261, 2011): SEEIRO rel. error vs iteration